Food Chemistry: X 20 (2023) 100984

Contents lists available at ScienceDirect

Food Chemistry: X

journal homepage: www.sciencedirect.com/journal/food-chemistry-x

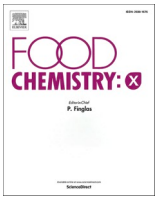

Effects of protein concentration, ionic strength, and heat treatment on the interfacial and emulsifying properties of coconut (*Cocos nucifera* L.) globulins

Jingrong Ma [a,1], Chuang Pan [b,1], Haiming Chen [a,*], Weijun Chen [a], Jianfei Pei [a], Ming Zhang [a], Qiuping Zhong [a], Wenxue Chen [a,*], Guangjin Zeng [c]

[a] HNU-HSF Collaborative Innovation Laboratory, College of Food Sciences & Engineering, Hainan University, 58 People Road, Haikou 570228, China
[b] Key Laboratory of Aquatic Product Processing, Ministry of Agriculture and Rural Affairs, National R&D Center for Aquatic Product Processing, South China Sea Fisheries Research Institute, Chinese Academy of Fishery Sciences, Guangzhou 510300, China
[c] Haikou Dongchang Pepper Co. LTD, China

ARTICLE INFO

Keywords:
Coconut globulins
Protein concentration
Ionic strength
Heat treatment
Interfacial properties
Emulsifying stability

ABSTRACT

This research aimed to investigate the effects of protein concentration (0.2 %-1.0 %), ionic strength (100–500 mM NaCl), and heat treatment (temperature: 80 and 90℃; time: 15 and 30 min) on the interfacial and emulsifying properties of coconut globulins (CG). When protein concentration was set at 0.2–0.6 %, the interfacial adsorption increased with the increasing of protein concentration. However, the lowest interfacial viscoelasticity was found when CG concentration was 0.6 %. When the protein concentration was higher than 0.6 %, the dilatational viscoelasticity increased with the increasing of protein concentration. The protein concentration showed positive effect on the emulsion stability of CG. The ionic strength showed positive effect on the interfacial adsorption but negative effects on the interfacial viscoelasticity and emulsion stability. Higher temperature and longer heating time brought worse interface behavior. The heated CG (90℃, 30 min) had the worst interfacial behavior but the best emulsion stability.

1. Introduction

Coconut proteins are essential tropical and subtropical plant proteins that have not been reported to cause food allergies (Kotecka-Majchrzak, Sumara, Fornal, & Montowska, 2020). As a natural emulsifier, it primarily mediates the stability of coconut milk. Therein, coconut globulins (CG) account for 40 % and play a major role in the good emulsifying activity (Patil & Benjakul, 2017). Emulsification is one of the most important functional properties of CG for utilization. However, the emulsifying properties of CG are far from being fully understood. Proteins could effectively stabilize emulsion through adsorbing and forming viscoelastic film at the oil–water interface. The interfacial behaviors of protein, including interfacial tension, interfacial adsorption, and viscoelasticity, are crucial for stabilizing emulsion (Amagliani & Schmitt, 2017; Cai et al., 2023; Felix, Romero, Carrera-Sanchez, & Guerrero, 2019; Ruiz-Alvarez, del Castillo-Santaella, Maldonado-Valderrama, Guadix, Guadix, & Garcia-Moreno, 2022; Sanchez & Patino, 2021; Yang & Sagis, 2021). However, studies on the interfacial properties of CG are not available so far. The study on the interfacial behavior of CG is conducive to better understanding the emulsifying properties and provides a guidance for the application.

Protein concentration, ionic strength, and temperature could significantly influence the interfacial behaviors of proteins (Nasrabadi, Doost, & Mezzenga, 2021; Pham, Tran, Ton, & Le, 2017; Tian, Taha, Zhang, Zhang, Hu, & Pan, 2021; Zhou, Tobin, Drusch, & Hogan, 2021). In the general case, increasing protein concentration positively improves the interfacial behavior and emulsifying activity of proteins (Liu & Tang, 2014). Tian et al. (2021) demonstrated that the interfacial properties and emulsifying efficiency of β-conglycinin significantly depend on the increase in protein concentration. However, Wang, Wang, Dai, Yu, and Cheng (2023) revealed that increasing the hemp seed protein concentration (1–3 %) would decrease the molecular rearrangement rate of hemp seed protein at the oil–water interface. The ionic strength could greatly influence the interfacial behavior of proteins since the ionic

* Corresponding authors.
E-mail addresses: hmchen168@126.com (H. Chen), hnchwx@163.com (W. Chen).
[1] These authors contributed equally to this work and should be regarded as co-first authors.

https://doi.org/10.1016/j.fochx.2023.100984
Received 31 May 2023; Received in revised form 5 October 2023; Accepted 6 November 2023
Available online 8 November 2023

strength could change the conformational state and net charges of proteins (Xiong, Li, Li, & Wang, 2019). Chang, Lan, Chen, and Rao (2023) unveiled that the enhanced electrostatic screening effect caused by NaCl could increase the interfacial adsorption but decrease the viscoelasticity of the interfacial layer of green pea protein. Heating above the denaturation temperature could dissociate protein structures, induce partial conformation unfolding, and result in subsequent aggregation (Ma, Wang, Wu, Xu, Du, & Wu, 2021; Wang et al., 2019). The heat-induced aggregation had significant influence on the interfacial properties of proteins. Shen et al. (2022) found that the heated (95 °C, 20 min) soy protein isolates showed a more significant apparent diffusion rate and a shorter equilibrium adsorption time. Ma et al. (2021) also investigated the effects of different temperatures (70-100℃) on the interfacial properties of cod proteins. They demonstrated that the preheat treatment could promote surface active properties and significantly increase the ratios of cod proteins-absorption at the oil–water interface.

Due to the close relationship between interfacial behavior and emulsion stability, it is necessary to study the emulsifying stability of CG by illuminating its interfacial properties. In previous researches, we have studied the physicochemical properties of CG at different temperatures and the interfacial behavior at different pH (Ma et al., 2022; 2023). However, the effects of protein concentration, ionic strength, and heat treatment (temperature and time) on the interfacial properties of CG haven't been illuminated. This study aimed to investigate the interfacial and emulsifying stability of CG at various protein concentrations, ionic strength, and heat treatment. First, the interfacial adsorption of CG was illuminated through dynamic interfacial tension and adsorption kinetics. Second, the interfacial viscoelastic properties were analyzed via linear and non-linear interfacial dilatational rheology. Last, the emulsifying stability of CG was characterized by droplet size distributions, zeta potential and centrifugal stability.

2. Materials & methods

2.1. Materials

Coconuts (Hainan Tall) were obtained from Wenchang city (Hainan, China). Medium-chain triglyceride (MCT) was purchased from Sports Research Co. (San Pedro, CA, U.S. A.). All reagents were of analytical grade unless otherwise specified.

2.2. Sample preparation

The CG powder (89 % protein, dry weight basis) was obtained according to the method described by Ma et al. (2022). Briefly, the albumin was removed by washing the de-fatted coconut meal with distilled water for 3 times, then the globulins were extracted using 0.5 M sodium chloride. The globulins were then dialyzed against 20 volumes of deionized water for 72 h (6–8 kDa molecular weight cut off). Dialysates were then freeze-dried to get the CG powder. The CG solutions were obtained by solubilizing the CG powder into 100 mL phosphate buffer (10.0 mM, pH 7.0). For studying the effects of protein concentration, the CG concentration was set at 0.2, 0.4, 0.6, 0.8, and 1.0 % (w/w), and the NaCl concentration was 300 mM. For studying the effects of ionic strength, the NaCl concentration was set at 100, 300, and 500 mM, and the CG concentration was 0.2 % (w/w). In addition, for studying the effects of heat treatment, 40 mL of CG solutions were heated in a water bath. The heating temperature was set at 80 and 90℃ (the sample temperature reached required values within 3 min), the heating time was 15 and 30 min, the CG concentration was 0.2 % (w/w), and the NaCl concentration was 300 mM. After heating, they were immediately cooled to 4℃ in an ice bath. The choice of denaturation temperature was based on previous studies on the physicochemical properties of CG (Ma et al., 2022). The obtained samples were stored at 4℃ before any further analysis.

2.3. Protein solubility determination

The protein solubility of CG was calculated as the ratio of soluble protein concentration and the total protein concentration (6500 g, 10 min, 25℃). The protein concentration was determined using a BCA Protein Assay Kit (Lian et al., 2023). The BCA Protein Assay Kit was purchased from Nanjing Jiancheng Bioengineering Institute (Nanjing, China). Mixing 250 μL test solution with 10 μL test sample and incubating at 37℃ for 30 min. Then, the absorbance value was measured at 562 nm. The bovine serum albumin (Solarbio, Beijing, China) was used as a standard to prepare the standard curve. The protein concentration was calculated as follows:

$C=(A_t-A_0)/(A_s-A_0) \times 0.524$;

where C is the protein concentration (mg/mL); A_t is the absorbance of test sample; A_s is the absorbance of standard protein; A_0 is the absorbance of buffer; 0.524 is the protein concentration of standard protein (mg/mL).

2.4. Interfacial properties analysis

The interfacial behaviors of CG solutions were evaluated by an optical contact anglemeter (OCA-20, Data-physics Instruments GmbH, Germany) as the method described by Niu, Chen, Luo, Chen, and Fu. (2022a) and Wan, Yang, and Sagis. (2016). The experiments were carried out at 25 °C. The CG samples were placed in the syringe and the oil phase (medium chain fatty acid, MCT) was placed in the cuvette. A drop of protein solution (20 μL) was delivered to the MCT oil and allowed to stand for 18000 s to achieve protein adsorption at the oil–water interface. A Charged Coupled Device (CCD) camera (PMS-Z65C-H12-W, Germany) and oscillating drop accessory (ODG-20) were used to record and digitalize the image of the sample drop continuously.

2.4.1. Dynamic interfacial tension and adsorption kinetics

The interfacial tension (γ) of the sample solution was calculated, and the interfacial pressure is π (mN/m) = γ_0-γ, where γ_0 is the interfacial tension of the buffer solution. The evolution of π versus time can be presented by Eq. (1) (Graham & Phillips, 1979):

$$\pi = 2C_0KT(Dt/3.14)^{1/2} \quad (1)$$

where C_0 is the sample concentration, K is the Boltzmann constant, T is the absolute temperature, D is the diffusion coefficient, and t is the time. As shown in Fig. 1b, the slope curve of π against $t^{1/2}$ is calculated as the diffusion rate (k_{diff}). In addition, the first-order rate equation (Eq. (2)) was used to characterize the interfacial penetration and reorganization of sample solutions (Graham & Phillips, 1979):

$$\ln(\pi_f-\pi_t)/(\pi_f-\pi_0) = -k_i t \quad (2)$$

Where π_f, π_t, and π_0 represent the interfacial pressures at the final time, any time and initial time, respectively. In addition, k_i is the first-order rate constant. The plot of $\ln[(\pi_f - \pi_t)/(\pi_f - \pi_0)]$ versus t has two linear regions (Fig. 1c): the first slope of this curve is designated as the penetration rate (K_p), the second slope represents the reorganization rate (K_r).

2.4.2. Dilatational rheological properties

The linear dilatational modulus was determined at the deformation amplitude of 10 % (ΔA/A) and frequency of 0.1 Hz, and the test time for each sample (20 μL) was 18000 s. The viscoelastic modulus (E) is composed of elasticity modulus (E_d) and viscosity modulus (E_v). $E_d = |E|\cos\delta$, $E_v = |E|\sin\delta$, where δ is the phase angle between stress and strain.

To reveal the rheological response at fast and large deformations, the non-linear surface dilatational rheology (frequency and amplitude sweep) was performed after 18000 s of equilibrium time. The frequency sweep was conducted with a stepwise increased frequency from 0.005 to

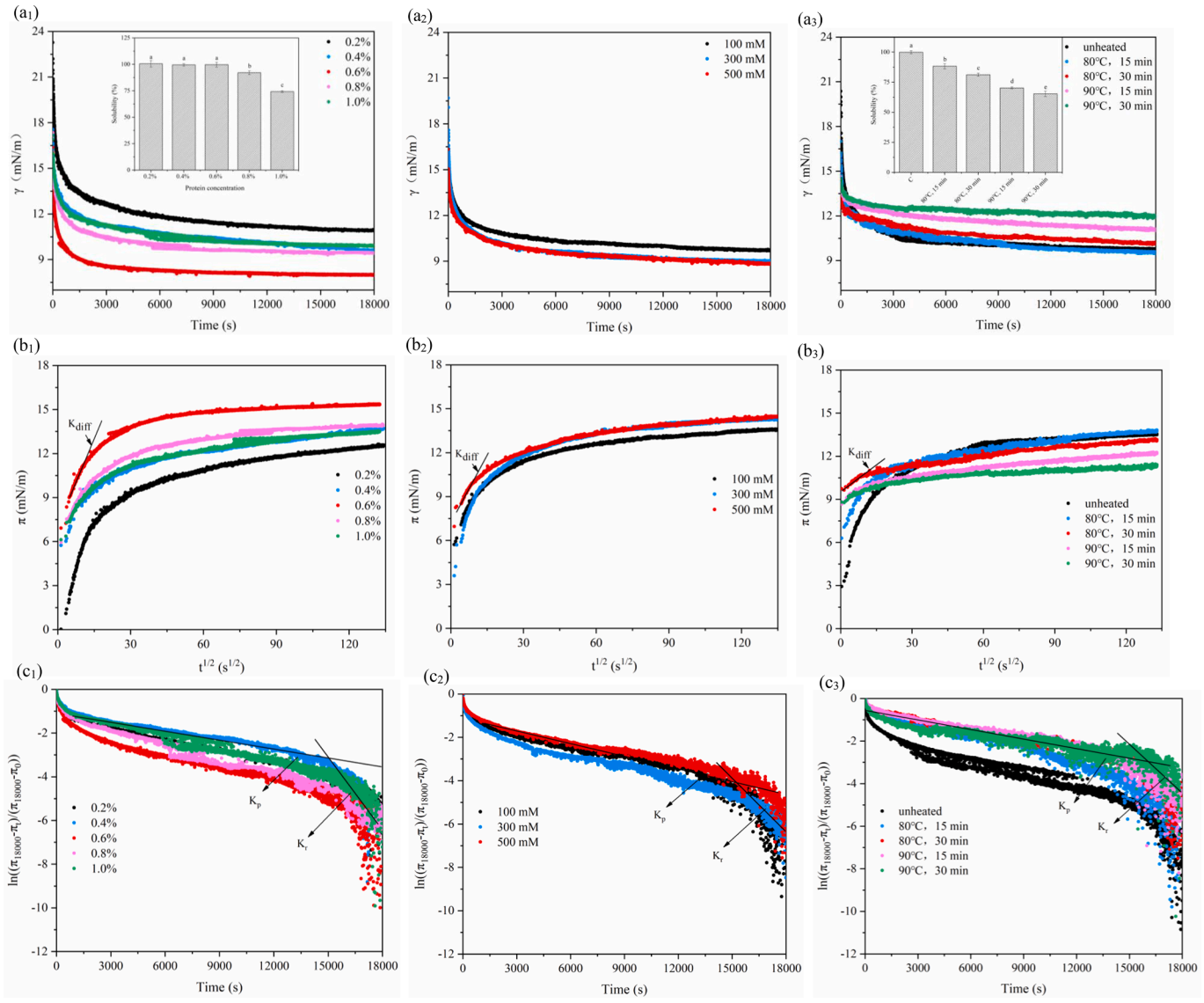

Fig. 1. (a_1-a_3) Effects of protein concentration(a_1), NaCl concentration(a_2), and heating (a_3) on the dynamic interfacial tension (γ) of CG at the oil–water interface, the insert picture in a_1 is the solubility of CG at different protein concentration. (b_1-b_3) Effects of protein concentration(b_1), NaCl concentration(b_2), and heating (b_3) on the $t^{1/2}$ -dependent π of CG at the oil–water interface, K_{diff} represents diffusion rate. (c_1-c_3) The profile of the molecular penetration and rearrangement steps at the oil–water interface of CG under different protein concentration(c_1), NaCl concentration(c_2), and heating (c_3), K_p and K_r represent first-order rate constants of penetration and rearrangement, respectively.

1 Hz, the amplitude was constant at 10 %. For amplitude sweep, it was performed at a deformation from 5 % to 30 % (ΔA/A) with a constant frequency of 0.1 Hz.

2.5. Preparation of emulsions

Oil-in-water emulsions with 10 % (v/v) MCT as a dispersed phase and 90 % (v/v) CG solution as a continuous. The mixture of MCT and CG solution was homogenized by high-speed dispersing with an Ultra-Turrax (IKA-25, Staufen, Germany) at 15,000 rpm for 2 min.

2.6. Stability analysis of emulsion

2.6.1. Determination of droplet size

Droplet sizes of the emulsions were tested by a laser analyzer (BT-9300ST, Baite Co. Ltd., China).

2.6.2. Zeta potential

The zeta potential was measured by a Zetasizer Nano-ZS instrument (Malvern Instruments, Worcestershire, UK). The emulsion samples were diluted 100 times with sodium phosphate buffer (10.0 mM, pH 7.0).

2.6.3. Centrifugal stability of emulsion

The emulsion stability was further analyzed by LUMiSizer stability analyzer (LUM GmbH, Berlin, Germany). The LUMiSize stability analyzer represents a time- and space-dependent transfer curve over the entire sample length under centrifugation. As the centrifugation time increased, the emulsion became unstable, the lighter oil droplets gradually migrated upward, while the heavier water phase stayed at the bottom of the sample tube. Therefore, the movement of emulsion particles is visualized by transmitted light intensity over time (Chen et al., 2023). The instrumental parameters: temperature, 25℃; wavelength, 870 nm; rotation speed, 4000 rpm; total centrifugation time, 50 min. Transmission profiles of the samples were drawn with the increase of separation time.

2.7. Statistical analysis

Unless specified otherwise, all tests were conducted in triplicate. An analysis of variance (ANOVA) was used to analyze significant differences ($p < 0.05$) through IBM SPSS 24.0 package (SPSS Inc., Chicago, USA). Besides, Duncan test was used for multiple comparisons.

3. Results and discussion

3.1. Interfacial adsorption

3.1.1. Dynamic surface tension

As shown in Fig. 1a, the γ values of all the samples gradually decreased with adsorption time (Fig. 1a), which could be explained by the interfacial adsorption. When the protein concentration is lower than 0.6 %, the dynamic γ decreased with the increasing of protein concentration (Fig. 1a1). CG with concentration of 0.6 % showed the lowest dynamic surface tension. Then, it increased with the increasing of protein concentration. This result was attributed to the protein solubility under different protein concentration. As shown in the insert figure in Fig. 1a1, the solubility of CG showed 100 % when protein concentration was between 0.2 % and 0.6 %. When the protein concentration was larger than 0.6 %, the solubility decreased significantly with the increasing of concentration. CG is a salt soluble protein and its ability to dissolve in solution is limited. The maximum amount of CG that can dissolve in the phosphate buffer (10.0 mM, pH 7.0, 300 mM NaCl) was 7.36 mg/mL (data were obtained from solubility results). The insoluble proteins at 0.8 % and 1.0 % would impede the interfacial adsorption of CG and then increase the dynamic γ. As shown in Fig. 1a2, the dynamic γ significantly decreased with the increase of NaCl concentration, which indicated that electrostatic screening (higher ionic strength) could lead to faster interfacial adsorption of CG (Tian et al., 2021). When the NaCl concentration increased from 300 mM to 500 mM, the dynamic γ only showed a slight decrease, which indicated that the electrostatic screening had saturated under 300 mM NaCl. The dynamic γ with different heat treatment is shown in Fig. 1a3. When heated at 80 °C for 15 min, the dynamic γ showed little change but increased obviously after heated for 30 min. The dynamic γ of 90℃ groups was significantly higher than 80℃ groups. As shown in Fig. 1a3 (insert), the solubility decreased significantly with the increase in heating temperature and time. Higher heating temperatures causes more protein aggregates, decreasing the protein solubility and interfacial adsorption (Yang, Liu, Zeng, & Chen, 2018). The CG heated at 90℃ for 30 min had the highest dynamic γ, which also confirmed that the protein aggregates would reduce the interfacial adsorption of CG.

3.1.2. Adsorption kinetics at the oil–water interface

The K_{diff}, K_p, and K_r of CG samples are summarized in Table 1. The K_{diff} of CG significantly decreased upon an increase in protein concentration, which indicated that CG with lower protein concentration is more easily diffusing at the interface. The concentration gradient and chemical potential gradient from interactions of the interface with the hydrophobic, electrostatic, hydration, and conformational potentials of proteins always act as driving force for interfacial diffusion (Zhou et al., 2021). For example, the concentration gradient is the driving forces for diffusion of highly soluble surfactants like polysaccharide and dairy protein (Kim, Wang, & Selomulya, 2020; Niu et al., 2022a; Zhou et al., 2021). However, the plant globulin is rigid with low solubility and strong electrostatic repulsion (Huang, Lee, Wang, & Qiu, 2023; Nasrabadi et al., 2021; Wang et al., 2012). Obviously, the influence of chemical potential gradient is greater than protein concentration for CG. When the protein concentration was low, the steric hindrance possessed by the limited CG proteins is weak, facilitating a higher diffusion of CG (Tian et al., 2021). As the c was increased, the increased steric hindrance hindered the diffusion of CG. For all the samples, the K_r values were considerably higher than K_p values, suggesting that the structural rearrangement of adsorbed CG dominates the formation of the interfacial layer rather than the penetration (Jia, Wang, Lu, Zheng, Zheng, & Guo, 2019). The K_r values of protein concentration at 0.2 and 0.4 % were higher than that of 0.6 %. It suggests that the protein has more space at the oil–water interface under low concentration, which is conducive for a rapid molecular rearrangement. Wang et al. (2023) also demonstrated that the K_r of hemp seed protein decreased with the increase of protein concentration. When the protein concentration was larger than 0.6 %, the insoluble proteins could increase the K_r values of CG. The CG with 300 mM NaCl showed the highest K_{diff}, followed by 500 and 100 mM NaCl. The higher ionic strength could lead electrostatic screening and then increase the diffusion and penetration of protein particles by reducing the energy barrier for adsorption. K_r showed a negative correlation with ionic strength indicating that the molecular interaction and reorganization of CG decreased due to the electrostatic screening effects. The K_{diff}, K_P, and K_r decreased with the increase of heating temperature and time. Different from the insoluble proteins in CG with protein concentration of 0.8 and 1.0 %, the heat-induced insoluble protein aggregates not only hindered the protein adsorption but also decreased the adsorption kinetics.

Table 1
Effects of protein concentration, NaCl concentration, and heating on the interfacial adsorption kinetics of CG. K_{diff}: diffusion rate; K_p: penetration rate; K_r: rearrangement rate.

		K_{diff} (mN/m/$s^{1/2}$)	$K_p \times 10^4$	$K_r \times 10^4$
protein concentration	0.2 %	0.652 ± 0.005[a]	−1.674 ± 0.015[d]	−8.479 ± 0.041[a]
	0.4 %	0.485 ± 0.009[b]	−1.327 ± 0.038[e]	−8.586 ± 0.056[a]
	0.6 %	0.446 ± 0.005[c]	−1.818 ± 0.024[c]	−6.788 ± 0.108[d]
	0.8 %	0.360 ± 0.006[d]	−2.165 ± 0.052[a]	−7.240 ± 0.089[c]
	1.0 %	0.305 ± 0.008[e]	−1.955 ± 0.007[b]	−8.209 ± 0.068[b]
NaCl concentration	100 mM	0.357 ± 0.016[c]	−1.581 ± 0.007[b]	−6.290 ± 0.108[a]
	300 mM	0.536 ± 0.007[a]	−1.849 ± 0.003[a]	−5.621 ± 0.048[b]
	500 mM	0.378 ± 0.012[b]	−1.536 ± 0.005[c]	−5.240 ± 0.111[c]
heating	unheated	0.573 ± 0.004[a]	−2.052 ± 0.029[a]	−11.057 ± 0.195[a]
	80℃, 15 min	0.355 ± 0.011[b]	−1.961 ± 0.033[b]	−8.485 ± 0.086[b]
	80℃, 30 min	0.111 ± 0.004[c]	−1.505 ± 0.008[c]	−7.850 ± 0.057[c]
	90℃, 15 min	0.106 ± 0.004[c]	−1.421 ± 0.007[d]	−5.540 ± 0.029[d]
	90℃, 30 min	0.086 ± 0.003[d]	−1.233 ± 0.003[e]	−5.413 ± 0.016[d]

Different lowercase letters within the same column are significant ($p < 0.05$) by Duncan's multiple range test.

3.2. Linear surface dilatational rheology

3.2.1. Viscoelasticity

The E-π curves were conducted to demonstrate the viscoelasticity of the interfacial layer. As shown in Fig. 2a1-3, the E increased with the interfacial pressure, indicating that the interfacial viscoelastic films were continuously formed. The slopes of the E-π curves were used to analyze the degree of interaction between CG molecules. The sharp slopes of the E-π curve correspond to stronger molecular interaction, which is crucial for forming viscoelastic interfacial layer (Choe et al., 2022). As shown in Fig. 2a1, at low protein concentrations (0.2–0.6 %), the slopes of the E-π curve decreased with the increase of concentration. This result indicated that the higher steric hindrance caused by high protein concentration is not conducive to protein interaction. When the

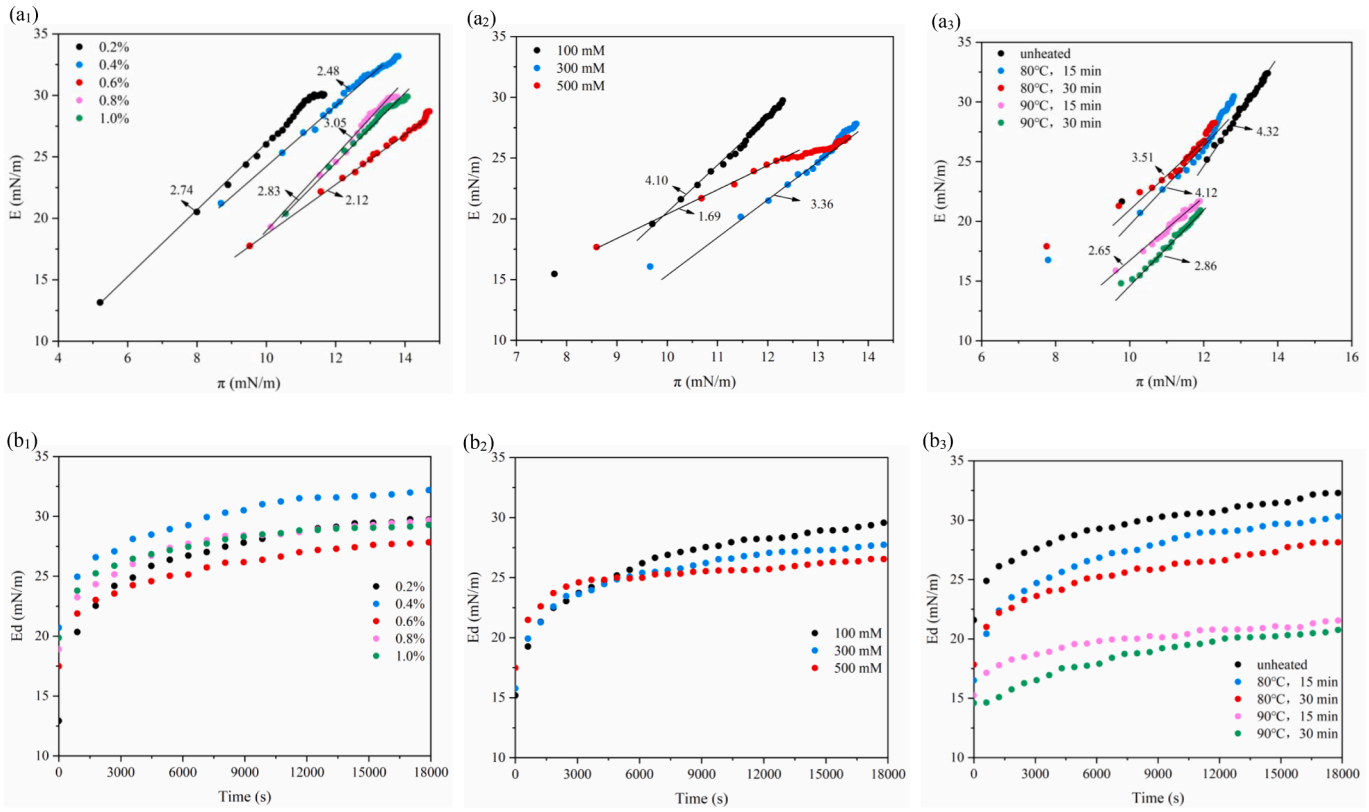

Fig. 2. (a_1-a_3) Effects of protein concentration(a_1), NaCl concentration(a_2), and heating (a_3) on the interface dilatational modulus (E) as a function of interface pressure (π) of CG at the oil–water interface. (b_1-b_3) Effects of protein concentration(b_1), NaCl concentration(b_2), and heating (b_3) on the time-dependent dilatational elasticity (E_d) of CG at the oil–water interface. Frequency: 0.1 Hz. Amplitude of compression/expansion cycle: 10 %.

protein concentration reached larger than 0.6 %, the insoluble proteins were slid to the oil–water interface with the extension and compression of the drop and then increased the molecular interaction. CG with 100 mM NaCl showed the highest E values and slopes, followed by 300 and 500 mM NaCl (Fig. 2a2). The electrostatic screening increased with the increasing of ionic strength; however, the molecular interaction is weakening. Tian et al. (2021) also found that a high ionic strength could decrease the electrostatic barrier for adsorption but hinder the intermolecular interaction of β-conglycinin. As shown in Fig. 2a3, the slope values decreased with the increase in heating temperature and time. The molecular interaction of CG at the oil–water interface was more significantly reduced when heated at 90℃ compared with 80℃.

3.2.2. *Elasticity*

The dilatational elastic modulus (E_d) results are presented in Fig. 2b1-3. The E_d values were verged on the E values (data not shown), which indicated that the interfacial layer of CG mainly displayed elastic properties (Wan, Wang, Wang, Zhou, Yuan, & Yang, 2014). As shown in Fig. 2b1, the E_d values with protein concentration at 0.2 and 0.4 % were higher than 0.6 %, which corresponded to the K_r values (Table 1). When the concentrations were higher than 0.6 %, the E_d values showed a positive correlation with the increase of protein concentration. Consistent with the results of slopes of the E-π curves, the E_d values were noticeably decreased with the increase of ionic strength (Fig. 2b2). In addition, the trend for E_d values corresponds to that of the K_r values (Table 1), which also indicated that the interfacial layer of CG was determined by the rearrangement. The lower intermolecular interactions led to the lower elastic properties, and the E_d of CG decreased with heat treatment (Fig. 2b3). Notably, the CG heated at 90℃ for 30 min exhibited the lowest E_d values.

3.3. *Non-linear surface dilatational rheology*

3.3.1. *Frequency sweep*

The results of the dilatational frequency sweep are shown in Fig. 3a1-3. Due to the exchange of the molecules between the surface layer and bulk solution and the in-plane structural reorganization on the surface layer, the dilatational modulus continuously increased with the frequency (Freer, Yim, Fuller, & Radke, 2004). As shown in Fig. 3a1, at low protein concentrations (0.2–0.6 %), the dilatational modulus decreased with the increase of concentration. CG showed the lowest dilatational modulus during frequency sweeps under the concentration of 0.6 %. When the concentration larger than 0.6 %, the dilatational modulus increased with the increase of protein concentration. The CG concentration at 1.0 % displayed the lowest solubility. However, it exhibited a higher dilatational modulus at high-frequency perturbation, which indicated that the high-frequency perturbation could promote the insoluble proteins to reach the interface. Similar to the results of linear surface dilatational rheology, the dilatational modulus during frequency sweep, all groups decreased with the increase of ionic strength (Fig. 3a2). As shown in Fig. 3a3, the heat treatment could significantly decrease the dilatational modulus of CG. Obviously, the CG heated 90℃ had lower E values than 80℃. This could be explained by the lower protein solubility of 90℃-heating, which decreased the interfacial adsorption. Moreover, more protein aggregates heated at 90℃ caused bigger physical barrier for the exchange of the molecules between the surface layer and bulk solution.

3.3.2. *Amplitude sweep*

The results of the viscoelastic modulus versus amplitude are shown in Fig. 3b1-3. The viscoelastic modulus decreased with the increase of amplitude, which indicated that the structures of the interfacial layers were damaged. The trend of interfacial viscoelasticity during amplitude

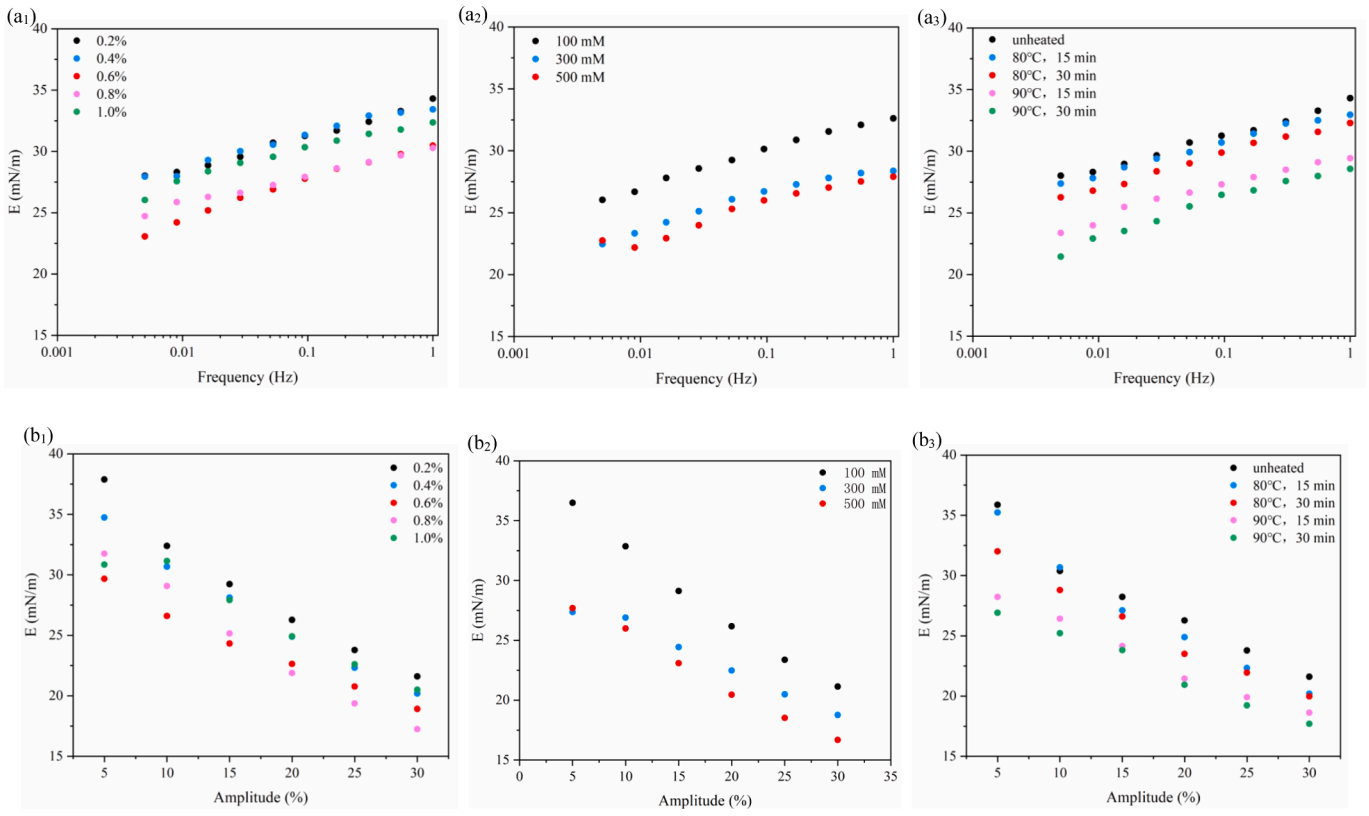

Fig. 3. (a_1-a_3) Complex surface dilatational modulus as a function of frequency for oil–water interfaces stabilized by CG under different protein concentration(a_1), NaCl concentration(a_2), and heating (a_3). Frequency: 0.005–1 Hz. Amplitude of deformation: 10 %. (b_1-b_3) Complex surface dilatational modulus as a function of amplitude for oil–water interfaces stabilized by CG under different protein concentration(b_1), NaCl concentration(b_2), and heating (b_3). Frequency: 0.1 Hz. Amplitude of deformation: 5–30 %.

sweep was similar to the results of the frequency sweep. As shown in Fig. 3b1, at low protein concentrations (0.2–0.6 %), the dilatational modulus of CG decreased with the increase of concentration. When the protein concentrations were higher than 0.6 %, the dilatational modulus increased with the increase of concentrations. The dilatational modulus of CG also decreased upon an increase in ionic strength under high amplitude perturbation (Fig. 3b2). As shown in Fig. 3b3, the dilatational modulus of CG decreased significantly after heating, demonstrating that the interfacial layer of heated CG is more easily be disturbed.

3.4. Emulsion stability

The droplet size distributions, zeta potential, and centrifugal stability of the emulsions were measured to characterize the emulsion stability. The influence of various protein concentrations on the droplet size distributions of the emulsion was not very significant. To some extent, there were more small droplet size distributions depending on the increase of protein concentrations (Fig. 4a1). As shown in Fig. 4a2, the influence of ionic strength on the droplet size distributions of the emulsion was also not very significant. The emulsion stabilized by CG with 500 mM NaCl showed more big droplet size distributions, indicating worse emulsion stability (Lee et al., 2021). At low ionic strength, there is a relatively strong electrostatic repulsion between the droplets, which helps prevent them coming into close contact. However, the electrostatic repulsion decreased with the increase of ionic strength, which is not conducive to the emulsion stability. Onsaard, Vittayanont, Srigam, and McClements (2005) pointed out a similar result that higher salt concentration would decrease the emulsion stability of coconut skim milk proteins. Tian et al. (2021) also found that the increases in ionic strength negatively affect the emulsifying efficiency of β-conglycinin. The heat treatment with different temperatures and times significantly influenced the emulsion's droplet size distributions (Fig. 4a3). Especially the emulsions stabilized by CG heated at 90℃ for 15 and 30 min showed smaller droplet size distributions, which indicated better emulsion stability. Sun, Chen, Chen, Zhong, Zhang, & Shen (2022) also demonstrated that the 90℃ preheating (20 min) gave coconut protein better emulsifying stability.

When the protein concentrations increased from 0.2 % to 1.0 %, the absolute value of zeta potential of the emulsion was increased from 14.93 to 16.27 (Fig. 4b1). This result suggested that high protein concentration could improve the net charges of emulsions, which is good for the emulsion stability to some degree since the higher zeta potential could stabilize the emulsion system well (Li et al., 2020). As shown in Fig. 4b2, the increase of in ionic strength caused electrostatic screening and then lead to significant decreases in the absolute value of zeta potentials ($p < 0.05$). As shown in Fig. 4b3, the heat treatment with different temperatures and times showed barely influences on the zeta potential, which indicated that the net charges are finite within CG. Obviously, the effect of heat treatment on the emulsifying stability of CG is not by changing the potential.

The emulsion stability of CG was further evaluated by the LUMiSize stability analyzer through accelerated centrifugation. As shown in Fig. 5, the transmission profiles (a_1- a_3) and instability indexes (b_1- b_3) of the emulsions were recorded. For the transmission profile, the bottom red line and top green line represented the first and last transmission profile, respectively. A thicker profiles and smaller transmission area represent a more stable emulsion (Niu, Chen, Luo, Chen, & Fu, 2022b). The value of instability index usually ranges from 0 to 1, where 0 means that the sample is not separated, and 1 means that the sample is completely separated (Niu et al., 2022a). The bigger instability index means worse emulsion stability. As shown in Fig. 5a1, the emulsion stability of CG was increased upon an increase in protein concentrations to some degree (with smaller instability index in Fig. 5b1). The thickness of the

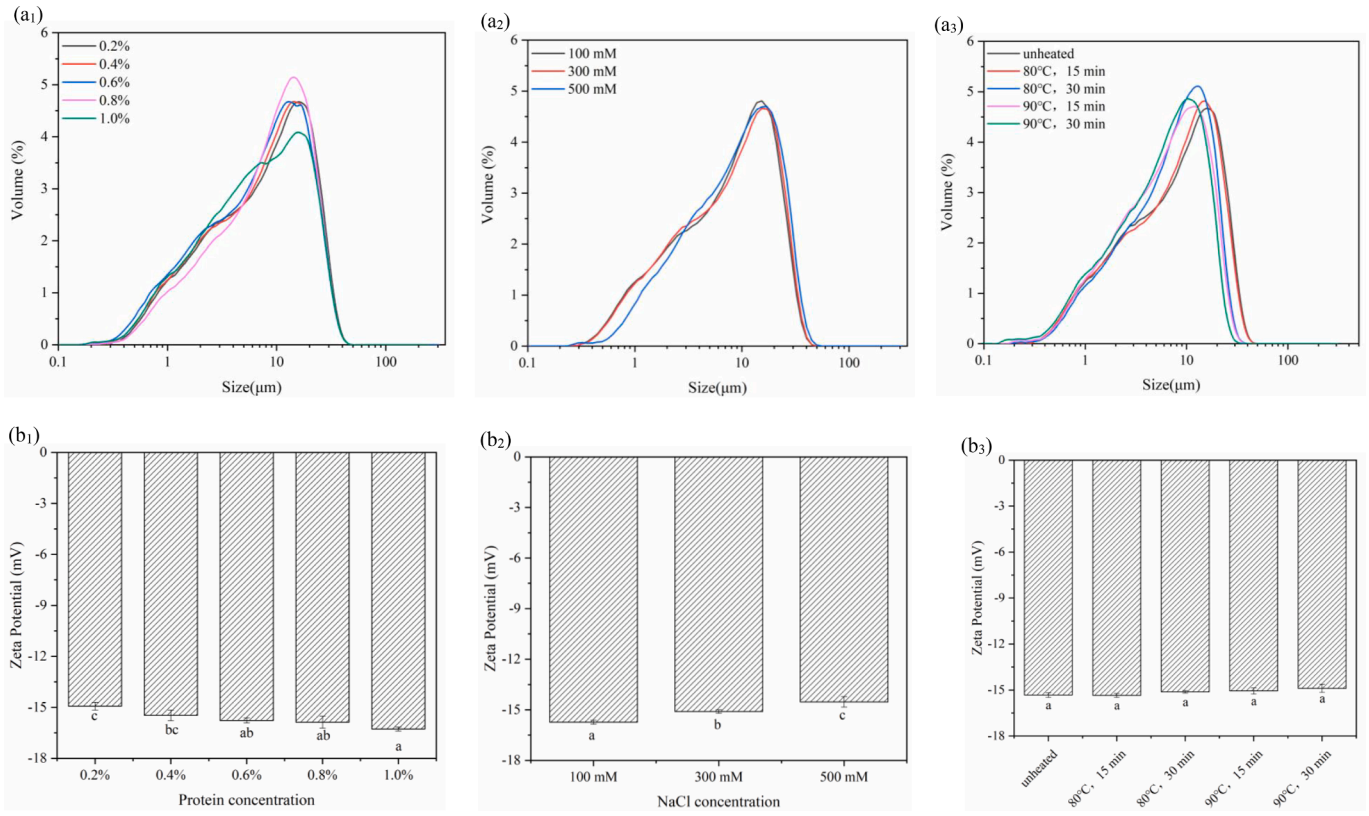

Fig. 4. (a_1-a_3) Particle size distribution of emulsions stabilized by CG under different protein concentration(a_1), NaCl concentration(a_2), and heating (a_3). (b_1-b_3) Zeta potential of emulsions stabilized by CG under different protein concentration(b_1), NaCl concentration(b_2), and heating (b_3).

transmission profiles decreased with the increase of ionic strength (Fig. 5a2). The higher ionic strength is not conducive to the emulsion stability of CG, which also shows up in the instability index (Fig. 5b2). Chang et al. (2023) also reported that increasing ionic strength weakened the emulsifying stability of green pea protein by decreasing the viscoelasticity of the interfacial layer. Overall, without modifying, changes of protein concentration and ionic strength did not considerably improve emulsion stability. As shown in Fig. 5a3 and 5b3, the emulsion stability of CG was increased upon an increase in heating temperature and time. Especially for the emulsion stabilized by CG heated at 90 ℃ for 30 min, it had the thickest transmission profiles and the lowest instability index.

3.5. Relationship between the interfacial behavior and emulsion stability of CG

At low protein concentrations (0.2–0.6 %), the interfacial adsorption and viscoelasticity increased and decreased with the increasing of protein concentrations, respectively. The insoluble proteins improved the interfacial rearrangement when the protein concentration was larger than 0.6 %. In addition, the viscoelasticity of the interface layer increased with the increase of concentrations, no matter with a linear or non-linear deformation. In general case, good interfacial behavior of emulsifiers corresponds to good emulsion stability (Niu et al., 2022a). However, the effect of protein concentrations on the interface behavior and emulsifying stability of CG do not correspond exactly. The emulsion stability of CG depends on the increase of concentration. Even though CG showed low solubility at high protein concentration, the insoluble proteins could assist to stabilize the emulsion by improving interfacial viscoelasticity and zeta potentials. The increase in ionic strength brought an increasing tendency to the interfacial adsorption, however, it is not conducive to the reorganization and the interfacial viscoelasticity of CG. The emulsion stability also decreased with the increase of ionic strength, which corresponded to the result of the interfacial viscoelasticity. This result indicated that the influence of interfacial viscoelasticity on the emulsion stability of CG is greater than that of interfacial adsorption when at a fixed concentration. Both the interfacial adsorption and viscoelasticity of CG were decreased with the increase in heating temperature and time. However, the emulsion stability increased significantly, which could be explained by the Pickering mechanism (Wang et al., 2022; Zhang et al., 2021). The heat-induced protein aggregates (especially heated at 90℃) could stabilize the emulsion by partial wettability between the oil–water phase (Kim, Wang, & Selomulya, 2020). Due to the protein aggregates are trapped between the two phases, they form a strong desorption energy barrier and a high particle adsorption barrier simultaneously, leading to a higher capillary force on both sides (Kim et al., 2020).

4. Conclusion

This work investigated the interfacial and emulsifying stability of CG at various protein concentrations, NaCl concentrations, and heat treatments. At low protein concentrations (0.2–0.6 %), the effect of protein concentration on interfacial adsorption and viscoelasticity is quite opposite. The CG had the best interfacial adsorption but the lowest interfacial viscoelasticity under the concentrations of 0.6 %. The insoluble proteins impeded the interfacial adsorption but improved the interfacial viscoelasticity when the protein concentration was larger than 0.6 %. The effect of protein concentrations on the interface behavior and emulsifying stability of CG do not correspond exactly. The emulsion stability depends on the increase of protein concentrations. The increase in ionic strength decreased the interfacial viscoelasticity and emulsifying stability of CG. The interface behavior of CG decreased with the increase in heating temperature and time, however, the emulsion stability was increased. When the protein concentration is 0.2 % (pH 7.0, 300 mM NaCl), heating at 90℃ for 30 min (solubility is

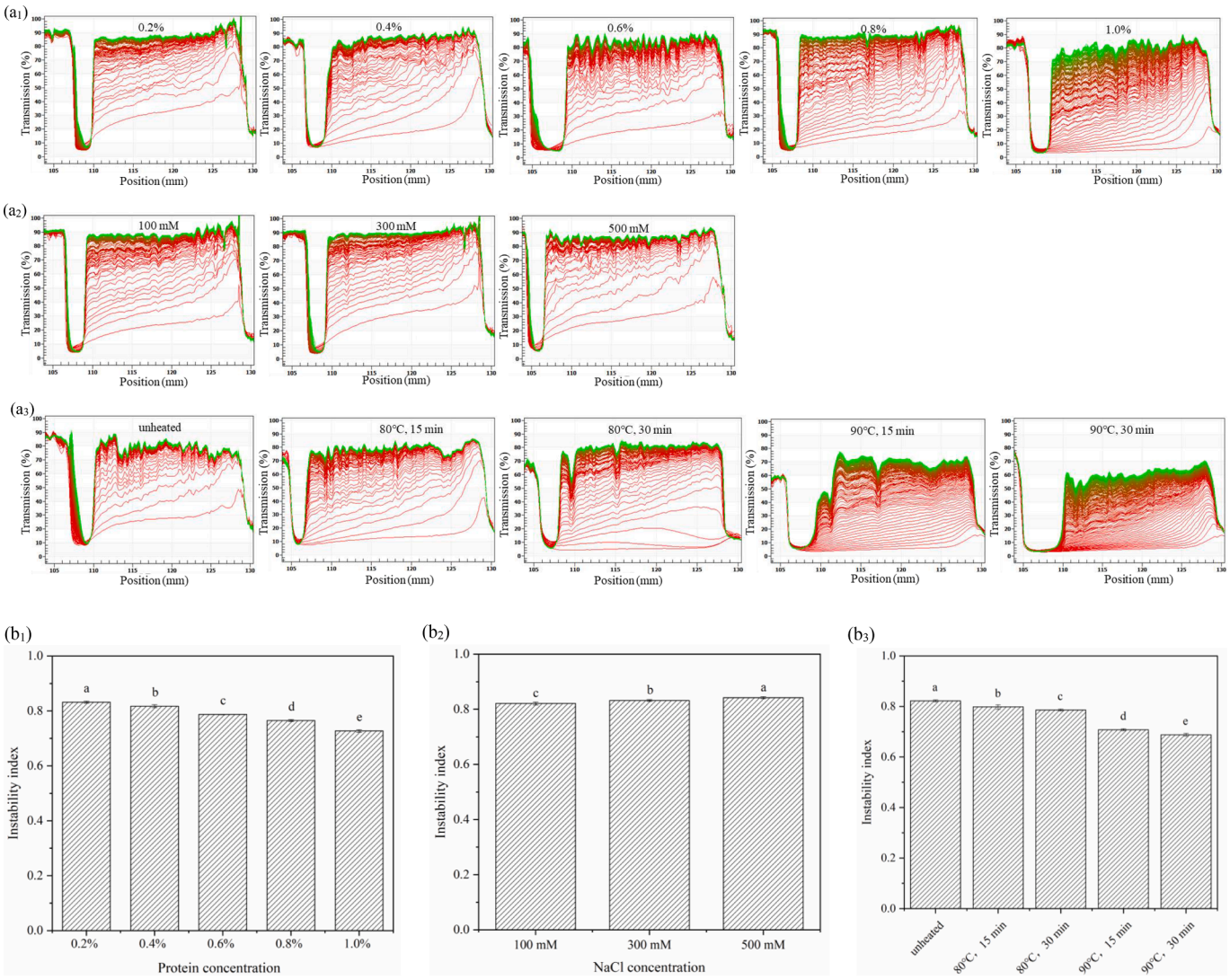

Fig. 5. (a_1-a_3) Transmission profile of emulsions stabilized by CG under different protein concentration(a_1), NaCl concentration(a_2), and heating (a_3). (b_1-b_3) Instability index of emulsions stabilized by CG under different protein concentration(b_1), NaCl concentration(b_2), and heating (b_3).

65.32 %) is a potential way to improve the emulsion stability of CG. This study helps us have a better understanding on the emulsifying properties of CG and provides a theoretical basis for its application in emulsion system.

CRediT authorship contribution statement

Jingrong Ma: Writing – original draft, Investigation. **Chuang Pan:** Writing – review & editing. **Haiming Chen:** Methodology, Resources. **Weijun Chen:** Data curation. **Jianfei Pei:** Validation. **Ming Zhang:** Supervision. **Qiuping Zhong:** Validation. **Wenxue Chen:** Project administration. **Guangjin Zeng:** Resources.

Declaration of Competing Interest

The authors declare that they have no known competing financial interests or personal relationships that could have appeared to influence the work reported in this paper.

Data availability

Data will be made available on request.

Acknowledgments

This work was supported by grants from Hainan Provincial Natural Science Foundation (322QN434), Hainan Province Science and Technology Special Fund (ZDYF2022XDNY166).

References

Amagliani, L., & Schmitt, C. (2017). Globular plant protein aggregates for stabilization of food foams and emulsions. *Trends in Food Science & Technology, 67*, 248–259.

Cai, Z., Wei, Y., Shi, A., Zhong, J., Rao, P., Wang, Q., & Zhang, H. (2023). Correlation between interfacial layer properties and physical stability of food emulsions: Current trends, challenges, strategies, and further perspectives. *Advances in Colloid and Interface Science, 313*, Article 102863.

Chang, L. Y., Lan, Y., Chen, B. C., & Rao, J. J. (2023). Interfacial, and emulsifying properties nexus of green pea protein fractions: Impact of pH and salt. *Food Hydrocolloids, 140*, Article 108652.

Chen, Y., Yao, M., Yang, T., Fang, Y., Xiang, D., & Zhang, W. (2023). Changes in structure and emulsifying properties of coconut globulin after the atmospheric pressure cold plasma treatment. *Food Hydrocolloids, 136*, Article 108289.

Choe, U., Chang, L., Ohm, J. B., Chen, B., & Rao, J. (2022). Structure modification, functionality and interfacial properties of kidney bean (Phaseolus vulgaris L.) protein concentrate as affected by post-extraction treatments. *Food Hydrocolloids, 133*, Article 108000.

Felix, M., Romero, A., Carrera-Sanchez, C., & Guerrero, A. (2019). Assessment of interfacial viscoelastic properties of Faba bean (Vicia faba) protein-adsorbed O/W layers as a function of pH. *Food Hydrocolloids, 90*, 353–359.

Freer, E. M., Yim, K. S., Fuller, G. G., & Radke, C. J. (2004). Shear and dilatational relaxation mechanisms of globular and flexible proteins at the hexadecane/water interface. *Langmuir, 20*(23), 10159–10167.

Graham, D., & Phillips, M. (1979). Proteins at liquid interfaces: III. Molecular structures of adsorbed films. *Journal of Colloid and Interface Science, 70*(3), 427–439.

Huang, Q. Q., Lee, Y. Y., Wang, Y., & Qiu, C. Y. (2023). Structural characterization, interfacial and emulsifying properties of soy protein hydrolysate-tannic acid complexes. *Food Hydrocolloids, 137*, Article 108415.

Jia, X. Z., Wang, J. Y., Lu, X., Zheng, B. X., Zheng, B. D., & Guo, Z. B. (2019). Structure and dilatational rheological behavior of heat-treated lotus (Nelumbo nucifera Gaertn.) seed protein. Lwt-Food. *Science and Technology, 116*, Article 108579.

Kim, W., Wang, Y., & Selomulya, C. (2020). Dairy and plant proteins as natural food emulsifiers. *Trends in Food Science & Technology, 105*, 261–272.

Kotecka-Majchrzak, K., Sumara, A., Fornal, E., & Montowska, M. (2020). Oilseed proteins - Properties and application as a food ingredient. *Trends in Food Science & Technology, 106*, 160–170.

Lee, H. W., Lu, Y. Y., Zhang, Y. Y., Fu, C. L., & Huang, D. J. (2021). Physicochemical and functional properties of red lentil protein isolates from three origins at different pH. *Food Chemistry, 358*, Article 129749.

Li, D., Zhao, Y., Wang, X., Tang, H., Wu, N., Wu, F., … Elfalleh, W. (2020). Effects of (+)-catechin on a rice bran protein oil-in-water emulsion: Droplet size, zeta-potential, emulsifying properties, and rheological behavior. *Food Hydrocolloids, 98*, Article 105306.

Lian, Z. T., Yang, S., Liao, P. L., Dai, S. C., Tong, X. H., Tian, T., … Jiang, L. Z. (2023). Emulsifying properties and oil-water interface properties of succinylated soy protein isolate: Affected by conformational flexibility of the interfacial protein. *Food Hydrocolloids, 136*, Article 108224.

Liu, F., & Tang, C. H. (2014). Emulsifying Properties of Soy Protein Nanoparticles: Influence of the Protein Concentration and/or Emulsification Process. *Journal of Agricultural and Food Chemistry, 62*(12), 2644–2654.

Ma, J. R., Chen, H. M., Chen, W. J., Wu, J. L., Li, Z. Q., Zhang, M., … Chen, W. X. (2022). Effects of heat treatment and pH on the physicochemical and emulsifying properties of coconut (Cocos nucifera L.) globulins. *Food Chemistry, 388*, Article 133031.

Ma, J. R., Pan, C., Chen, H. M., Chen, Y., Chen, W. J., Pei, J. F., … Chen, W. X. (2023). Interfacial behavior of coconut (Cocos nucifera L.) globulins at different pH: Relation to emulsion stability. *Food Hydrocolloids, 144*, Article 108958.

Ma, W. C., Wang, J. M., Wu, D., Xu, X. B., Du, M., & Wu, C. (2021). Effects of preheat treatment on the physicochemical and interfacial properties of cod proteins and its relation to the stability of subsequent emulsions. *Food Hydrocolloids, 112*, Article 106338.

Nasrabadi, M. N., Doost, A. S., & Mezzenga, R. (2021). Modification approaches of plant-based proteins to improve their techno-functionality and use in food products. *Food Hydrocolloids, 118*, Article 106789.

Niu, H., Chen, X. W., Luo, T., Chen, H. M., & Fu, X. (2022a). The interfacial behavior and long-term stability of emulsions stabilized by gum arabic and sugar beet pectin. *Carbohydrate Polymers, 291*, Article 119623.

Niu, H., Chen, X. W., Luo, T., Chen, H. M., & Fu, X. (2022b). Relationships between the behavior of three different sources of pectin at the oil-water interface and the stability of the emulsion. *Food Hydrocolloids, 128*, Article 107566.

Onsaard, E., Vittayanont, M., Srigam, S., & McClements, J. (2005). Properties and Stability of Oil-in-Water Emulsions Stabilized by Coconut Skim Milk Proteins. *Journal of Agricultural and Food Chemistry, 53*(14), 5747–5753.

Patil, U., & Benjakul, S. (2017). Characteristics of albumin and globulin from coconut meat and their role in emulsion stability without and with proteolysis. *Food Hydrocolloids, 69*, 220–228.

Pham, T. T., Tran, T. T. T., Ton, N. M. N., & Le, V. V. M. (2017). Effects of pH and salt concentration on functional properties of pumpkin seed protein fractions. *Journal of Food Processing and Preservation, 41*(4), e13073.

Ruiz-Alvarez, J. M., del Castillo-Santaella, T., Maldonado-Valderrama, J., Guadix, A., Guadix, E. M., & Garcia-Moreno, P. J. (2022). pH influences the interfacial properties of blue whiting (M. poutassou) and whey protein hydrolysates determining the physical stability of fish oil-in-water emulsions. *Food Hydrocolloids, 122*, Article 107075.

Sanchez, C. C., & Patino, J. M. R. (2021). Contribution of the engineering of tailored interfaces to the formulation of novel food colloids. *Food Hydrocolloids, 119*, Article 106838.

Shen, Q., Xiong, T., Zheng, W., Luo, Y., Peng, W., Dai, J., … Chen, Y. (2022). The effects of thermal treatment on emulsifying properties of soy protein isolates: Interfacial rheology and quantitative proteomic analysis. *Food Research International, 157*, Article 111326.

Sun, Y. Z., Chen, H. M., Chen, W. X., Zhong, Q. P., Zhang, M., & Shen, Y. (2022). Effects of Ultrasound Combined with Preheating Treatment to Improve the Thermal Stability of Coconut Milk by Modifying the Physicochemical Properties of Coconut Protein. *Foods, 11*(7), 1042.

Tian, Y., Taha, A., Zhang, P. P., Zhang, Z., Hu, H., & Pan, S. Y. (2021). Effects of protein concentration, pH, and NaCl concentration on the physicochemical, interfacial, and emulsifying properties of beta-conglycinin. *Food Hydrocolloids, 118*, Article 106784.

Wan, Z. L., Wang, L. Y., Wang, J. M., Zhou, Q., Yuan, Y., & Yang, X. Q. (2014). Synergistic interfacial properties of soy protein-stevioside mixtures: Relationship to emulsion stability. *Food Hydrocolloids, 39*, 127–135.

Wan, Z. L., Yang, X. Q., & Sagis, L. M. C. (2016). Nonlinear Surface Dilatational Rheology and Foaming Behavior of Protein and Protein Fibrillar Aggregates in the Presence of Natural Surfactant. *Langmuir, 32*(15), 3679–3690.

Wang, J. M., Xia, N., Yang, X. Q., Yin, S. W., Qi, J. R., He, X. T., & Wang, L. J. (2012). Adsorption and dilatational rheology of heat-treated soy protein at the oil-water interface: Relationship to structural properties. *Journal of Agricultural and Food Chemistry, 60*(12), 3302–3310.

Wang, M. P., Chen, X. W., Jian, G., Yang, J., Wang, J. M., & Yang, X. Q. (2019). Stabilization of foam and emulsion by subcritical water-treated soy protein: Effect of aggregation state. *Food Hydrocolloids, 87*, 619–628.

Wang, C., Wu, J., Wang, C., Mu, C., Ngai, T., & Lin, W. (2022). Advances in Pickering emulsions stabilized by protein particles: Toward particle fabrication, interaction and arrangement. *Food Research International, 157*, Article 111380.

Wang, T., Wang, N., Dai, Y. J., Yu, D. Y., & Cheng, J. J. (2023). Interfacial adsorption properties, rheological properties and oxidation kinetics of oleogel-in-water emulsion stabilized by hemp seed protein. *Food Hydrocolloids, 137*, Article 108402.

Xiong, W. F., Li, J., Li, B., & Wang, L. F. (2019). Physicochemical properties and interfacial dilatational rheological behavior at air-water interface of high intensity ultrasound modified ovalbumin: Effect of ionic strength. *Food Hydrocolloids, 97*, Article 105210.

Yang, J., & Sagis, L. M. C. (2021). Interfacial behavior of plant proteins - novel sources and extraction methods. *Current Opinion in Colloid & Interface Science, 56*, Article 101499.

Yang, J. Q., Liu, G. Y., Zeng, H. B., & Chen, L. Y. (2018). Effects of high pressure homogenization on faba bean protein aggregation in relation to solubility and interfacial properties. *Food Hydrocolloids, 83*, 275–286.

Zhang, T., Xu, J., Chen, J., Wang, Z., Wang, X., & Zhong, J. (2021). Protein nanoparticles for Pickering emulsions: A comprehensive review on their shapes, preparation methods, and modification methods. *Trends in Food Science & Technology, 113*, 26–41.

Zhou, B. B., Tobin, J. T., Drusch, S., & Hogan, S. A. (2021). Dynamic adsorption and interfacial rheology of whey protein isolate at oil-water interfaces: Effects of protein concentration, pH and heat treatment. *Food Hydrocolloids, 116*, Article 106640.